

**Figure 2.** Double potential step MCD (DPS/MCD) experiments of cytochrome *c*. Results shown were signal averaged 100 times, wavelength 417 nm: (a) ferricytochrome *c* 355  $\mu$ M in pH 7 Tris/cacodylic acid buffer ( $\mu = 0.2$ ); (b) ferrocyclochrome *c* 250  $\mu$ M in pH 7 Tris/cacodylic acid buffer ( $\mu = 0.2$ ). Magnetic field: 15 kg.

finding that  $k_2$  is less than  $k_1$ , i.e., the rate of conformational change following reduction is faster than the rate following oxidation.

MCD experiments were conducted as were the CD experiments described above. Figure 2a shows the experimental and simulated results with the bulk solution species being ferricytochrome *c*. Figure 2b shows the analogous results for a sample of ferrocyclochrome *c*. Again, when simulated responses (smooth solid line with dots) were compared with experimental data, best fits were found for the values  $k_1 \geq 50 \text{ s}^{-1}$  and  $k_2 = 20 \text{ s}^{-1}$ . The rate constant for the Cyt(III)\*  $\rightarrow$  Cyt(III) conformational change is found to be larger when monitored by MCD ( $k_2 = 20 \text{ s}^{-1}$ ) versus CD ( $k_2 = 10 \text{ s}^{-1}$ ). This is not surprising. The CD of the Soret band reflects the changes in the chiral environment of the heme moiety while the MCD is more sensitive to changes occurring in the coordination sphere of the metal ion.<sup>19</sup> Both CD and MCD are sensitive to the conformational changes of cytochrome *c* upon reduction and oxidation. However, MCD is more sensitive than CD to localized structural changes such as those that would be associated with changes in the iron-sulfur bond occurring upon electron transfer. Other conformational changes may then be propagated through the protein from the immediate environment about the heme following electron transfer. The differences in the rates of conformational change as observed here by CD and MCD are consistent with this view.

In conclusion, the experiments described here provide a means of studying the kinetics of conformational change of heme proteins during both reductive and oxidative electron-transfer reactions. Detailed studies of binding effects and pH effects on the conformational changes of cytochrome *c* during electron-transfer reactions are being pursued.

**Acknowledgment.** We greatly acknowledge the financial support of this work by the National Science Foundation, CHE-8520270 (F.M.H.) and the Ministry of Education, Science and Culture International Scientific Research Program, No. 02045033 (I.T.).

(19) Holmquist, B. In *The Porphyrins*, Dolphin, D., Ed.; Academic Press: New York, 1978; Vol. III, Chapter 5.

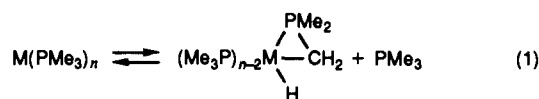
## Hexakis(trimethylphosphine)tungsten(0): Synthesis, Structure, and Reactivity

Daniel Rabinovich and Gerard Parkin\*

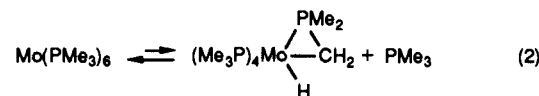
Department of Chemistry, Columbia University  
New York, New York 10027

Received February 23, 1990

Zerovalent homoleptic trimethylphosphine complexes,  $M(\text{PMe}_3)_n$ , have been isolated for several of the transition metals, including Mo, Fe, Os, Co, Ni, Pd, and Pt.<sup>1</sup> Interest in these complexes arises from the strong  $\sigma$ -donor coupled with weak  $\pi$ -acceptor properties of the trimethylphosphine ligand, a combination that generates metal centers in which the valence electrons are of high energy. Such metal complexes are often termed "electron rich" and show great promise for activating normally unreactive substances by oxidative addition, e.g. alkane C-H bonds.<sup>1b,2</sup> A consequence of the high reactivity of the metal centers in  $M(\text{PMe}_3)_n$  complexes is the facile formation of cyclometalated divalent derivatives accompanied by elimination of  $\text{PMe}_3$  (eq 1).<sup>1,3</sup> For example,  $\text{Mo}(\text{PMe}_3)_6$  has been shown to be in



equilibrium with low concentrations of the complex  $\text{Mo}(\text{PMe}_3)_4(\eta^2\text{-CH}_2\text{PMe}_2)\text{H}$  and  $\text{PMe}_3$  (eq 2).<sup>1a,b</sup> However, the



analogous tungsten complex,  $\text{W}(\text{PMe}_3)_6$ , has so far remained elusive. Attempts to prepare  $\text{W}(\text{PMe}_3)_6$  by both the co-condensation of tungsten atoms with  $\text{PMe}_3$  and the reduction of  $\text{WCl}_6$  with alkali metal reducing agents with  $\text{PMe}_3$  as a reactive solvent resulted in the isolation of the cyclometalated product  $\text{W}(\text{PMe}_3)_4(\eta^2\text{-CH}_2\text{PMe}_2)\text{H}$  in each case.<sup>3a-c</sup> Here we report that  $\text{W}(\text{PMe}_3)_6$  can indeed be isolated, and we describe the synthesis, structure, and kinetics and thermodynamics of its conversion to  $\text{W}(\text{PMe}_3)_4(\eta^2\text{-CH}_2\text{PMe}_2)\text{H}$ .

$\text{W}(\text{PMe}_3)_6$  is isolated as a yellow crystalline solid in good yield (>50%) by the reduction of  $\text{WCl}_6$  with Na(K) alloy with  $\text{PMe}_3$  as a reactive solvent (eq 3),<sup>4</sup> using a similar procedure to that

(1) (a) Brookhart, M.; Cox, K.; Cloke, F. G. N.; Green, J. C.; Green, M. L. H.; Hare, P. M.; Bashkin, J.; Derome, A. E.; Grebenik, P. D. *J. Chem. Soc., Dalton Trans.* **1985**, 423-433. (b) Cloke, F. G. N.; Cox, K. P.; Green, M. L. H.; Bashkin, J.; Prout, K. *J. Chem. Soc., Chem. Commun.* **1982**, 393-394. (c) Ermer, S. P.; Shinomoto, R. S.; Deming, M. A.; Flood, T. C. *Organometallics* **1989**, *8*, 1377-1378. (d) Klein, H.-F.; Karsch, H. H. *Chem. Ber.* **1975**, *108*, 944-955. (e) Klein, H.-F. *Angew. Chem., Int. Ed. Engl.* **1980**, *19*, 362-375. (f) Karsch, H. H.; Klein, H.-F.; Schmidbaur, H. *Angew. Chem., Int. Ed. Engl.* **1975**, *14*, 637-638. (g) Karsch, H. H.; Klein, H.-F.; Schmidbaur, H. *Chem. Ber.* **1977**, *110*, 2200-2212. (h) Timms, P. L. *Angew. Chem., Int. Ed. Engl.* **1975**, *14*, 273-277. (i) Rathke, J. W.; Muetterties, E. L. *J. Am. Chem. Soc.* **1975**, *97*, 3272-3273. (j) Ugo, R. *Coord. Chem. Rev.* **1968**, *3*, 319-344. (k) Malatesta, L.; Cenini, S. *Zerovalent Compounds of Metals*; Academic Press: New York, 1974.

(2) (a) Green, M. L. H.; O'Hare, D. *Pure Appl. Chem.* **1985**, *57*, 1897-1910. (b) Cloke, F. G. N.; Fyne, P. J.; Gibson, V. C.; Green, M. L. H.; Ledoux, M. J.; Perutz, R. N.; Dix, A.; Gourdon, A.; Prout, K. *J. Organomet. Chem.* **1984**, *277*, 61-73. (c) Shinomoto, R. S.; Desrosiers, P. J.; Harper, G. P.; Flood, T. C. *J. Am. Chem. Soc.* **1990**, *112*, 704-713.

(3) Metalated derivatives of the constitution  $M(\text{PMe}_3)_4(\eta^2\text{-CH}_2\text{PMe}_2)\text{H}$  have been reported for Mo, W, Fe, Ru, and Os. (a) Gibson, V. C.; Grebenik, P. D.; Green, M. L. H. *J. Chem. Soc., Chem. Commun.* **1983**, 1101-1102. (b) Gibson, V. C.; Graimann, C. E.; Hare, P. M.; Green, M. L. H.; Bandy, J. A.; Grebenik, P. D.; Prout, K. *J. Chem. Soc., Dalton Trans.* **1985**, 2025-2035. (c) Green, M. L. H.; Parkin, G.; Chen, M.; Prout, K. *J. Chem. Soc., Dalton Trans.* **1986**, 2227-2236. (d) Werner, H.; Gotzig, J. *Organometallics* **1983**, *2*, 547-549. (e) Gotzig, J.; Werner, R.; Werner, H. *J. Organomet. Chem.* **1985**, *290*, 99-114. (f) Werner, H.; Werner, R. *J. Organomet. Chem.* **1981**, *209*, C60-C64. (g) Graimann, C. E.; Green, M. L. H. *J. Organomet. Chem.* **1984**, *275*, C12-C14.

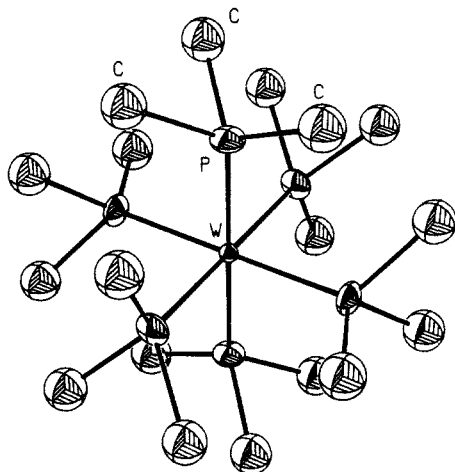
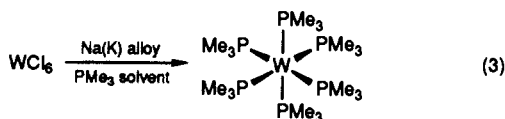
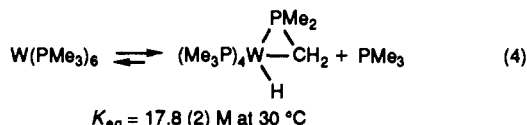


**Figure 1.** ORTEP diagram of  $W(PMe_3)_6$ . Selected bond distances and angles:  $W-P = 2.455(5)$  Å;  $P-W-P = 90$  and  $180^\circ$ .

reported for the preparation of  $W(PMe_3)_4(\eta^2-CH_2PMe_2)H$ .<sup>3a-c,8</sup> The molecular structure of  $W(PMe_3)_6$  has been determined by X-ray diffraction methods, as shown in Figure 1.<sup>5</sup>



Although  $W(PMe_3)_6$  may be stored for prolonged periods ( $>2$  weeks) at room temperature in the solid state, in solution  $W(PMe_3)_6$  is unstable and is converted rapidly to an equilibrium mixture with  $W(PMe_3)_4(\eta^2-CH_2PMe_2)H$  and  $PMe_3$  (eq 4). At



the concentration levels of  $PMe_3$  that are generated by the dissociation (typically  $\sim 5$ – $10$  mM), the reaction is effectively irreversible and proceeds to completion with a half-life of ca. 2 h at room temperature. However, in the presence of a large excess of added  $PMe_3$ , the position of equilibrium is shifted toward  $W(PMe_3)_6$  so that both  $W(PMe_3)_6$  and  $W(PMe_3)_4(\eta^2-CH_2PMe_2)H$  may be observed by  $^1\text{H}$  NMR spectroscopy, thereby allowing determination of the equilibrium constant,  $K_{eq}(30^\circ\text{C}) = 17.8(2)$  M. The temperature dependence of  $K_{eq}$  over the range  $30$ – $70^\circ\text{C}$  has allowed determination of  $\Delta H^\circ$  and  $\Delta S^\circ$  to be  $9.3(8)$  kcal  $\text{mol}^{-1}$  and  $37(2)$  eu, respectively, thus demonstrating that the reaction is driven entropically by dissociation of  $PMe_3$ .<sup>6</sup>

The mechanism proposed for the formation of  $W(PMe_3)_4(\eta^2-CH_2PMe_2)H$  involves rate-determining dissociation of  $PMe_3$  from  $W(PMe_3)_6$  to give the 16-electron intermediate  $[W(PMe_3)_5]$ ,

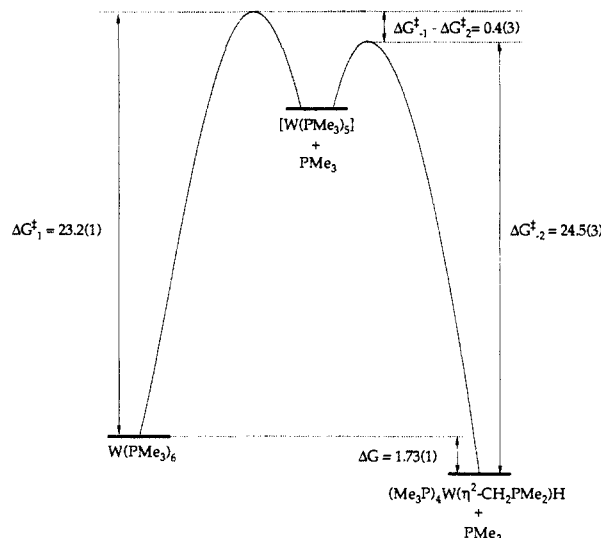
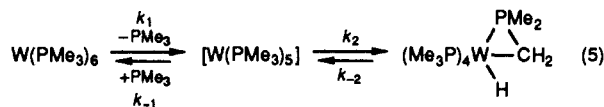


**Figure 2.** Free energy surface connecting  $W(PMe_3)_6$  to  $W(PMe_3)_4(\eta^2-CH_2PMe_2)H$  and  $PMe_3$  (values in kcal  $\text{mol}^{-1}$ ).

followed by rapid metalation of a C–H bond of one of the  $PMe_3$  ligands (eq 5). In accord with this mechanism, the conversion



of  $W(PMe_3)_6$  to  $W(PMe_3)_4(\eta^2-CH_2PMe_2)H$  is inhibited by addition of excess  $PMe_3$ . Kinetic studies have allowed determination of (i)  $k_1$ , the rate constant for dissociation of  $PMe_3$  from  $W(PMe_3)_6$ , (ii)  $k_2$ , the rate constant for reductive elimination of the  $[W](\eta^2-CH_2PMe_2)H$  unit, and (iii) the ratio of  $k_{-1}$  and  $k_2$ , i.e. the competition between coordination of  $PMe_3$  versus intramolecular oxidative addition of the C–H bond to the 16-electron species,  $[W(PMe_3)_5]$ . At  $30^\circ\text{C}$  these have the values  $k_1 = 1.2(1) \times 10^{-4} \text{ s}^{-1}$  ( $\Delta G^\ddagger_{30^\circ\text{C}} = 23.2(1)$  kcal  $\text{mol}^{-1}$ ),  $k_2 = 1.3(5) \times 10^{-5} \text{ s}^{-1}$  ( $\Delta G^\ddagger_{30^\circ\text{C}} = 24.5(3)$  kcal  $\text{mol}^{-1}$ ), and  $k_{-1}/k_2 = 0.5(2)$   $\text{M}^{-1}$ , as illustrated in Figure 2. At the low concentration levels of  $PMe_3$  ( $\sim 5$ – $10$  mM) that are generated during the course of the reaction in the absence of added  $PMe_3$ , the ratio  $k_{-1}[PMe_3]/k_2$  is sufficiently small ( $\sim 10^{-2}$ – $10^{-3}$ ) so that intramolecular C–H bond activation by  $[W(PMe_3)_5]$  is greatly favored over coordination of  $PMe_3$ . Under these conditions the rate-determining step is specifically dissociation of  $PMe_3$  from  $W(PMe_3)_6$ , for which measurement of the kinetics over the temperature range  $30$ – $60^\circ\text{C}$  have allowed the activation parameters  $\Delta H^\ddagger = 27.6(6)$  kcal  $\text{mol}^{-1}$  and  $\Delta S^\ddagger = 14(3)$  eu to be determined. Although the barrier for  $PMe_3$  dissociation from  $W(PMe_3)_6$  ( $E_a = 28.2(6)$  kcal  $\text{mol}^{-1}$ ) to form the 16-electron intermediate  $[W(PMe_3)_5]$  is comparable to that observed for  $PMe_3$  dissociation from the related complex  $Os(PMe_3)_5$  ( $E_a \approx 28$  kcal  $\text{mol}^{-1}$ ),<sup>1c,2c</sup> the barrier for formation of the 16-electron intermediate  $[M(PMe_3)_{n-1}]$  ( $M = W, n = 6$ ;  $M = Os, n = 5$ ) by reductive elimination of the C–H bond of the cyclometalated derivatives  $[M(PMe_3)_{n-2}(\eta^2-CH_2PMe_2)H]$  is significantly greater for Os than for W.<sup>7</sup>

In conclusion, the homoleptic tungsten complex  $W(PMe_3)_6$  may be readily obtained by the reduction of  $WCl_6$  with Na(K) alloy in  $PMe_3$  solvent. Dissociation of  $PMe_3$  from  $W(PMe_3)_6$  is facile and results in the formation of the metalated complex  $W(PMe_3)_4(\eta^2-CH_2PMe_2)H$ , with which it is in equilibrium.

(7) Although the barriers for reductive elimination ( $\Delta G^\ddagger_{30^\circ\text{C}} = 24.5(3)$  kcal  $\text{mol}^{-1}$  for  $W(PMe_3)_4(\eta^2-CH_2PMe_2)H$ ;  $\Delta G^\ddagger_{155^\circ\text{C}} \approx 37$  kcal  $\text{mol}^{-1}$  for  $Os(PMe_3)_3(\eta^2-CH_2PMe_2)H$ ) cannot be compared quantitatively since the experiments were carried out at different temperatures, the relative ease of the two processes is clearly indicated.

(8) **Note Added in Proof:**  $W(PMe_3)_6$  has also been observed as a partially characterized product, obtained in low yield by reduction of  $W(N-2,6-Pr'_2C_6H_3)Cl_4$  with Na sand in  $PMe_3$  solvent. Gibson, V. C.; Mitchell, J. P. Personal communication.

(4) A mixture of  $WCl_6$  (5 g) and Na(K) alloy (1:3 w/w, 5 g) in  $PMe_3$  (40 mL) was stirred at room temperature for 10 days. The  $PMe_3$  was removed in vacuo and the product was extracted into pentane ( $6 \times 300$  mL) at room temperature (ca. 30 min per extraction). After each extraction the filtrate was immediately concentrated, without warming, and allowed to cool to below room temperature. The extracts were combined and further concentrated to ca. 30 mL to give  $W(PMe_3)_6$  as a yellow microcrystalline solid (4.3 g, 53%) that was isolated in pure form, free from  $W(PMe_3)_4(\eta^2-CH_2PMe_2)H$ , by filtration. The filtrate consisted of a mixture of  $W(PMe_3)_4(\eta^2-CH_2PMe_2)H$  and  $W(PMe_3)_6$ . Note that in order to isolate  $W(PMe_3)_6$  in preference to  $W(PMe_3)_4(\eta^2-CH_2PMe_2)H$ , rapid extraction procedures are required. NMR data for  $W(PMe_3)_6$  (in  $C_6D_6$ ):  $^1\text{H}$   $\delta$  1.49, s;  $^{13}\text{C}\{^1\text{H}\}$   $\delta$  33.3, triplet of quintets,  $^1J_{C-P} \approx ^3J_{C-P(\text{trans})} \approx 2$  Hz,  $^3J_{C-P(\text{cis})} \approx 4$  Hz;  $^{31}\text{P}\{^1\text{H}\}$  (relative to  $\text{H}_3\text{PO}_4$ )  $\delta$   $-41.5$ , s,  $^1J_{P-W} = 294$  Hz. Anal. Found for  $C_{18}H_{34}P_6W$ : C, 33.8; H, 9.3. Calcd: C, 33.8; H, 8.5.

(5) Crystal data for  $W(PMe_3)_6$ : cubic,  $Im\bar{3}m$  (No. 229),  $a = 11.303(2)$  Å,  $V = 1444.1(6)$  Å<sup>3</sup>,  $Z = 2$ ,  $\rho(\text{calcd}) = 1.47$  g  $\text{cm}^{-3}$ ,  $\mu(\text{Mo K}\alpha) = 45.6$   $\text{cm}^{-1}$ ,  $\lambda(\text{Mo K}\alpha) = 0.71073$  Å (graphite monochromator); 351 unique reflections with  $3^\circ < 2\theta < 65^\circ$  were collected of which 247 reflections with  $F_o > 6\sigma(F_o)$  were used in refinement;  $R = 5.29\%$ ,  $R_w = 6.45\%$ , GOF = 1.165.

(6) Standard states of the components are 1 M.

**Supplementary Material Available:** Tables of crystal and intensity collection data, atomic coordinates, bond distances and angles, and anisotropic displacement parameters and an ORTEP drawing for  $W(\text{PMe}_3)_6$  (4 pages); listing of observed and calculated structure factors (2 pages). Ordering information is given on any current masthead page.

### Observation of a Cis Amide Isomer within a Linear Peptide

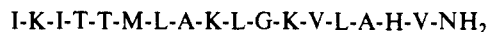
Eleni Bairaktari,<sup>†</sup> Dale F. Mierke,<sup>‡</sup> Stefano Mammi, and Evaristo Peggion\*

Biopolymer Research Center  
Department of Organic Chemistry, University of Padua  
Via Marzolo 1, 35131 Padua, Italy

Received December 26, 1989

Recently we initiated an examination of the conformational preferences of bombolitins, a series of peptides isolated from bumble bee venom.<sup>1</sup> Bombolitins exhibit biological profiles within membrane environments similar to those of mastoparan,<sup>2</sup> melittin,<sup>3</sup> and crabrolin,<sup>4</sup> in spite of the low sequence homology. All of these peptides are related in the amphiphilic nature of the  $\alpha$ -helices that they can form. In order to investigate the structures and determine a possible mechanism for activity, we are studying the peptides in the presence of SDS micelles as a mimic for a biological membrane.<sup>5,6</sup> During the NMR investigation of one of the bombolitins, bombolitin I, we observed the presence of a cis amide bond between the first and second residues, Ile<sup>1</sup> and Lys<sup>2</sup>. To our knowledge this is the first report of a cis amide within a linear peptide without a proline.<sup>7</sup>

Bombolitin I is a heptadecapeptide with the following sequence:



The proton NMR resonances of the peptide were assigned from phase-sensitive COSY, DQ correlated spectroscopy, and HOHAHA experiments.<sup>8,9</sup> The sequential assignment of the residues was achieved by NOESY spectra.<sup>10</sup>

In aqueous solution bombolitin I is random; all of the NOEs are indicative of conformational averaging. This is also borne out

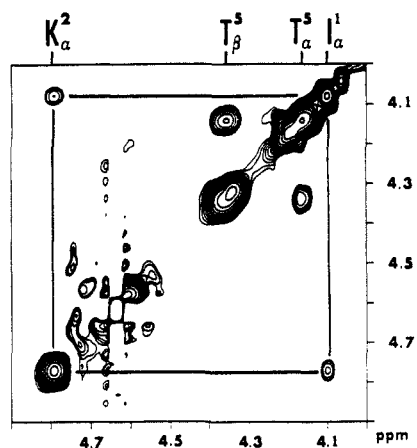


**Figure 1.** The aliphatic region of a pure-phase absorption NOESY spectrum (mixing time 200 ms) at 400 MHz of bombolitin I (2.6 mM with 320 mM SDS- $d_{25}$ ) in  $^2\text{H}_2\text{O}$ . The NOE demonstrating the cis  $\omega$ -bond between Ile<sup>1</sup> and Lys<sup>2</sup> [ $\text{C}^\alpha\text{H}(1) \rightarrow \text{C}^\alpha\text{H}(2)$ ] is illustrated. The other connectivity present arises from an intraresidue interaction.

with circular dichroism studies.<sup>6</sup> The nominal backbone NOEs observed throughout the peptide indicate that all of the amide linkages are in a trans arrangement. In contrast, in the presence of SDS above the critical micellar concentration (CMC), the peptide adopts a well-defined  $\alpha$ -helix. Characteristic NOEs [e.g.,  $\text{NH}(i) \rightarrow \text{NH}(i+1)$  and  $\text{C}^\alpha\text{H}(i) \rightarrow \text{C}^\beta\text{H}(i+3)$ ]<sup>11</sup> are quite conclusive; a long stretch of helix extending from residue 2 to at least residue 14 is present. This finding is in agreement with CD results.<sup>6</sup>

In addition to the characteristic NOEs, there is one observation that is highly unusual. The strong Ile<sup>1</sup>  $\text{C}^\alpha\text{H} \rightarrow$  Lys<sup>2</sup>  $\text{C}^\alpha\text{H}$  NOE demonstrates a cis arrangement about the Ile<sup>1</sup>–Lys<sup>2</sup> amide bond.<sup>12</sup> This result is illustrated in Figure 1. The two diagnostic peaks for a cis amide bond are  $\text{C}^\alpha\text{H}(i) \rightarrow \text{C}^\alpha\text{H}(i+1)$  and  $\text{NH}(i) \rightarrow \text{C}^\alpha\text{H}(i+1)$ .<sup>11,12</sup> Only the former is observed here due to fast exchange of the free amino group of Ile<sup>1</sup>.

The proton NMR spectrum of bombolitin I in the presence of SDS exhibits a single set of resonances for each amino acid. No trace of the trans amide isomer was detected. Considering also the CD results that indicate that the peptide is completely bound to micelles,<sup>6</sup> we conclude that a single conformation is assumed by bombolitin I upon association with SDS.

The cis  $\omega$ -bond must arise from the association of the peptide with the micelles and the amphiphilic nature of the  $\alpha$ -helix formed within this environment. Although our results do not allow for insight into the interaction of the peptide with the micelles, a favorable array would have the  $\alpha$ -helix on the surface of the micelle with the hydrophobic face directed into the surfactant and the hydrophilic face into the aqueous solution. Only with a cis arrangement can the side chains of isoleucine and lysine point toward opposite sides with Ile<sup>1</sup> interacting with the hydrocarbons of the micelles and Lys<sup>2</sup> with the water.

This study clearly indicates that the membrane can have a dramatic effect on the conformation of a peptide and underlines the importance of examining peptides within environments similar to the conditions wherein they exhibit activity. Peptide–membrane interactions can be energetically more important than the steric constraints usually associated with the cis arrangement (i.e., cis 2–3 kcal/mol higher in energy than trans). This result supports the role of membranes as mediators in the interactions of peptides with their receptors.

Registry No. Bombolitin I, 95648-97-8.

(11) Wüthrich, K.; Billeter, M.; Braun, W. *J. Mol. Biol.* **1984**, *180*, 715–740.

(12) Arseniev, A. S.; Knodakov, V. I.; Maiorov, V. N.; Volkova, T. M.; Grishin, E. V.; Bystrov, V. F.; Ovchinnikov, Y. A. *Bioorg. Khim.* **1983**, *9*, 768–793.

\* To whom correspondence should be addressed.

<sup>†</sup> Present address: Laboratory of Analytical Biochemistry, University Hospital, Ioannina, Greece.

<sup>‡</sup> Present address: Organisch-Chemisches Institut, Technische Universität München, Garching, FRG.

(1) Argiolas, A.; Pisano, J. J. *J. Biol. Chem.* **1985**, *260*, 1437–1444.

(2) Hirai, Y.; Yasuhara, T.; Yoshida, H.; Nakajima, T.; Fujino, M.; Kitada, C. *Chem. Pharm. Bull. (Tokyo)* **1979**, *27*, 1942–1944.

(3) Habermann, E. *Science* **1972**, *117*, 314–322.

(4) Argiolas, A.; Pisano, J. J. *J. Biol. Chem.* **1984**, *259*, 10106–10111.

(5) Bairaktari, E.; Bewley, C. A.; Mammi, S.; Peggion, E. In *Proceedings of the Eleventh American Peptide Symposium*; Rivier, J., Ed.; ESCOM: Leiden; pp 578–581.

(6) Bairaktari, E.; Mierke, D. F.; Mammi, S.; Peggion, E., in preparation.

(7) Configurational isomers with cis amide linkages have been reported within cyclic peptides: Mierke, D. F.; Yamazaki, T.; Said-Nejad, O. E.; Felder, E. R.; Goodman, M. *J. Am. Chem. Soc.* **1989**, *111*, 6847–6849.

(8) Two-dimensional NMR spectra were recorded with 256–512 experiments of 2K data points on a Bruker AM 400 instrument at 40 °C at a concentration of 2.6 mM bombolitin I, 10 mM phosphate buffer at pH 4.1 in  $^2\text{H}_2\text{O}$  (Aldrich) or in  $\text{H}_2\text{O}$  (10%  $^2\text{H}_2\text{O}$ ). The SDS samples contained 0.32 M SDS- $d_{25}$  (MSD Isotopes).

(9) The two-dimensional homonuclear Hartman–Hahn (HOHAHA) spectra were obtained by using the sequence described by Bax and Davis: Bax, A.; Davis, D. G. *J. Magn. Reson.* **1985**, *65*, 355–360. Double quantum (DQ) correlated spectra were recorded with a preparation period of 15 ms as described by Maceri and Freeman: Maceri, T. H.; Freeman, R. *J. Magn. Reson.* **1983**, *51*, 531–535.

(10) The NOESY spectra were acquired by using the standard sequence: Bodenhausen, G.; Kogler, H.; Ernst, R. R. *J. Magn. Reson.* **1984**, *58*, 370–388. Mixing times were varied from 75 to 200 ms.